Journal of the Optical Society of America B
OPTICAL PHYSICS

# Modal analysis of spatial pattern formation in fused silica under ultraviolet irradiation

DAVID A. EDWARDS[1,*] AND RICHARD O. MOORE[2]

[1]Department of Mathematical Sciences, University of Delaware, Newark, Delaware 19716, USA
[2]Department of Mathematical Sciences, New Jersey Institute of Technology, Newark, New Jersey 07102, USA
*Corresponding author: dedwards@udel.edu

Received 26 April 2016; revised 27 June 2016; accepted 27 June 2016; posted 28 June 2016 (Doc. ID 263869); published 18 July 2016

**Focused laser light is used as part of the photolithography process. Finer-resolution applications demand smaller-wavelength light, but this higher-energy light causes compaction of the lens glass. This changes its index of refraction, eventually rendering the lens unusable. The underlying model requires the use of Maxwell's equations with a varying index of refraction coupled to a nonlinear constitutive compaction law. By modeling the light wave in the paraxial limit, one obtains a nonlocal partial integrodifferential equation for the amplitude. Stability analysis is performed in the steady and quasi-steady cases, and the results show how the instability depends on physical parameters in the problem. The results compare favorably with experimental analyses of the failure length and time scales and provide simple laws connecting the relevant failure scales.** 

***OCIS codes:*** (220.3740) Lithography; (220.3630) Lenses; (140.3440) Laser-induced breakdown; (140.3610) Lasers, ultraviolet; (350.1820) Damage; (160.6030) Silica.

http://dx.doi.org/10.1364/JOSAB.33.001709

## 1. INTRODUCTION

Photolithography is an important process used in the fabrication of microchips and integrated circuits. Silicon wafers are etched with photosensitive chemicals. A series of chemical treatments then either engraves the exposure pattern into the wafer or enables deposition of a new material in the desired pattern. Repeating this process many times (tens to hundreds of cycles) allows for the creation of highly complex integrated circuits. Fused silica lenses are used to steer and focus laser light used in this process.

As transistor densities have increased, the need for finer etching resolution has grown as well. This increase has pushed the industry to use smaller-wavelength light, which comes with an increase in photon energy. Excimer lasers, which operate solely within the UV range (100–300 nm), are used extensively in the semiconductor industry. At these wavelengths, photon energies are high enough to interact with silica molecules in the lens.

Even at moderate intensities, exposure to this ultraviolet energy permanently compacts (densifies) the glass. These effects (local changes in density, physical shrinkage of lens material) develop after millions of pulses [1], which (given a normal duty of 1000 pulses/sec) correspond to time scales as short as a few hours.

Moreover, local changes in the lens density $\rho$ even on the order of parts-per-million (such as those imparted by UV–silica interactions) are significant enough to measurably affect optical characteristics, in particular, by changing the local index of refraction. This in turn causes interference through refractive gradients and nanometer changes in path length from physical shrinkage of the lens (see Fig. 1).

Due to photolithography's increasingly stringent resolution requirements, any degradation in beam quality is highly undesirable. A better understanding of laser/material interactions of UV photons within silica lenses could lead to ways to mitigate or eliminate the damage mechanism.

The proposed mechanism of these changes is through two-photon absorption. On their own, UV photons lack the necessary energy to interact meaningfully with silica molecules. However, if two photons collide with an atom at once, the simultaneous energy transfer is enough to change the orientation of the silica molecules into a tighter packed, more locally dense arrangement. This is referred to as "densification" or "compaction" in the literature [2,3]. These local changes in density create material stresses within the lens where the compressive forces of the densified regions generate tension with the unaffected material around them (see bottom of Fig. 1). Densification is an accumulative process that continues as the lens is used; thus, lens stress continues to grow over time.

Under certain conditions, an even more dramatic effect called "microchanneling" can occur. Experimental observations show that a few months to a year after a lens has begun densifying, small cylindrical voids on the order of microns (called microchannels) begin to form. They are parallel to the beam,

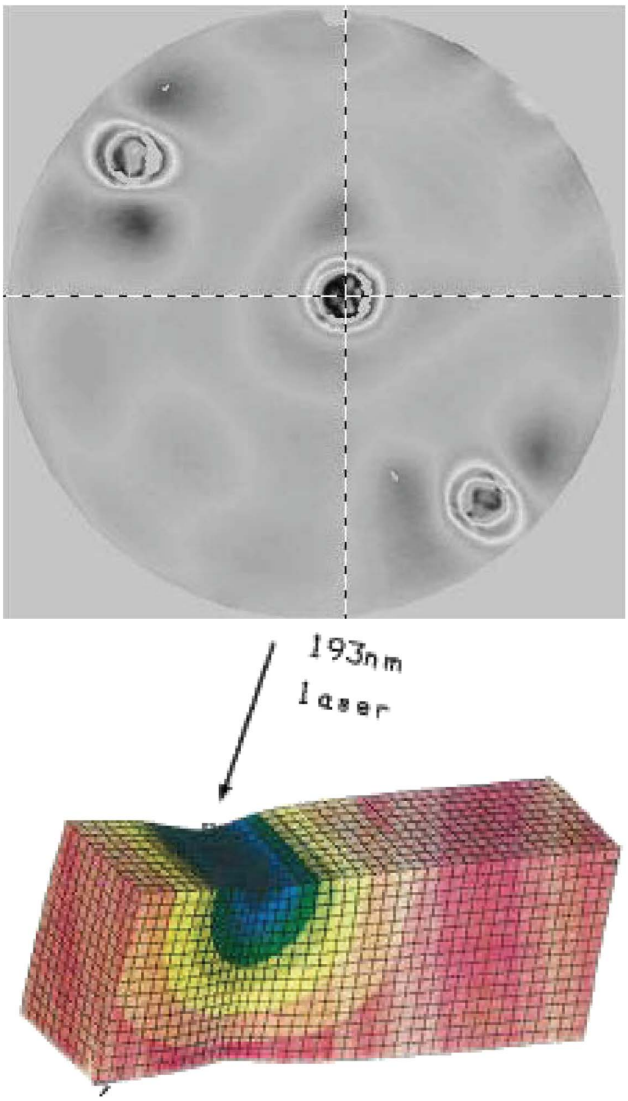


**Fig. 1.** Lens damage due to UV irradiation. Top: An interferogram showing stress birefringence [1]. Bottom: Contours of isostrain in a finite element simulation [5].

are much smaller in diameter than the beam at the exit face of the lens, and grow toward the front [1] (see Fig. 2).

At this time, the mechanism for microchannel formation is unknown, along with any causal relationship to the earlier densification process. We hypothesize that there is a feedback mechanism connecting the compaction and microchanneling phenomena. In particular, a steady transverse nonuniformity in the beam will create transverse and axial intensity gradients within the medium. Over a long time scale, these gradients can cause compaction, which changes the refractive index. This feedback loop can then cause self-focusing, intensity enhancement, and ultimately damage in the form of microchanneling.

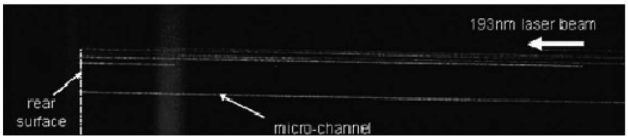


**Fig. 2.** Formation of microchannels at the exit face [1].

In this paper, we model the physical system using Maxwell's equations with a nonuniform index of refraction. The changes in the index of refraction are coupled to the intensity through a nonlinear constitutive law. The resulting nonlinear amplitude equation exhibits rich behavior. We examine both the quasi-steady and unsteady cases. The analysis leads directly to results that indicate how the solutions depend on physical parameters in the problem. Our estimates for the onset of damage compare favorably with experimental results.

## 2. GOVERNING EQUATIONS

To remind the reader of the additional terms that result from a varying refractive index, we briefly derive the governing equations from first principles. In the absence of free charges and currents, Maxwell's equations in an isotropic medium (assuming unit permeability) are given by [4, section 7.2]

$$\tilde{\nabla}\cdot\tilde{\mathbf{D}}=0,\qquad \tilde{\nabla}\cdot\tilde{\mathbf{B}}=0, \tag{1a}$$

$$\tilde{\nabla}\times\tilde{\mathbf{E}}=-\frac{1}{c}\frac{\partial\tilde{\mathbf{B}}}{\partial\tilde{t}}, \tag{1b}$$

$$\tilde{\mathbf{D}}=n^2(\tilde{\mathbf{E}})\tilde{\mathbf{E}}, \tag{1c}$$

$$\tilde{\nabla}\times\tilde{\mathbf{H}}=\frac{1}{c}\frac{\partial\tilde{\mathbf{D}}}{\partial\tilde{t}},\qquad \tilde{\mathbf{B}}=\tilde{\mathbf{H}}, \tag{1d}$$

where $\tilde{\mathbf{E}}$ and $\tilde{\mathbf{B}}$ are the electric and magnetic fields, respectively, $\tilde{\mathbf{D}}$ and $\tilde{\mathbf{H}}$ are the displacement and magnetizing fields, respectively, and $c$ is the speed of light.

Combining Eqs. (1c) and (1d) gives

$$\tilde{\nabla}\times\tilde{\mathbf{B}}=\frac{1}{c}\frac{\partial(n^2\tilde{\mathbf{E}})}{\partial\tilde{t}}. \tag{2}$$

Next, substituting Eq. (2) into the curl of Eq. (1b), we obtain

$$\tilde{\nabla}\times\tilde{\nabla}\times\tilde{\mathbf{E}}=\tilde{\nabla}(\tilde{\nabla}\cdot\tilde{\mathbf{E}})-\tilde{\nabla}^2\tilde{\mathbf{E}}=-\frac{1}{c^2}\frac{\partial^2(n^2\tilde{\mathbf{E}})}{\partial\tilde{t}^2},$$

where the middle term is a vector identity [6, section 10.31]. Substituting Eq. (1c) into the first of Eq. (1a) yields

$$\tilde{\nabla}\cdot\tilde{\mathbf{E}}=-\frac{1}{n^2}\tilde{\mathbf{E}}\cdot\tilde{\nabla}n^2.$$

Thus, the generic PDE for $\tilde{\mathbf{E}}$ is given by

$$\tilde{\nabla}\left(\frac{1}{n^2}\tilde{\mathbf{E}}\cdot\tilde{\nabla}n^2\right)+\tilde{\nabla}^2\tilde{\mathbf{E}}=\frac{1}{c^2}\frac{\partial^2(n^2\tilde{\mathbf{E}})}{\partial\tilde{t}^2}. \tag{3}$$

We expect that changes in $n$ due to the light wave will be small; therefore, we write

$$n=n_0+\delta n, \tag{4}$$

where $n_0$ is the uniform background index and where we consider $\delta n$ to be small. Substituting Eq. (4) into Eq. (3) and neglecting terms that are $O((\delta n)^2)$, we have

$$\tilde{\nabla}\left(\frac{1}{n_0^2}\tilde{\mathbf{E}}\cdot\tilde{\nabla}(2n_0\delta n)\right)+\tilde{\nabla}^2\tilde{\mathbf{E}}=\frac{1}{c^2}\frac{\partial^2((n_0^2+2n_0\delta n)\tilde{\mathbf{E}})}{\partial\tilde{t}^2}. \tag{5}$$

We consider a system where the glass occupies the half-space $\tilde{z} > 0$ and that incident upon it is a transverse plane wave $\tilde{\mathbf{E}} = \tilde{E}\mathbf{i}$, where $\mathbf{i}$ is the unit vector in the $\tilde{x}$ direction. Though in reality laser beams usually have Gaussian shape, damage occurs well before the Rayleigh length [7], making the plane-wave assumption a good first approximation.

Substituting our plane-wave assumption into Eq. (5), we obtain

$$\frac{2}{n_0}\frac{\partial}{\partial\tilde{x}}\left(\tilde{E}\frac{\partial(\delta n)}{\partial\tilde{x}}\right)+\frac{\partial^2\tilde{E}}{\partial\tilde{x}^2}+\frac{\partial^2\tilde{E}}{\partial\tilde{y}^2}+\frac{\partial^2\tilde{E}}{\partial\tilde{z}^2}=\frac{1}{c^2}\frac{\partial^2((n_0^2+2n_0\delta n)\tilde{E})}{\partial\tilde{t}^2}. \tag{6}$$

Next, allowing for slow variations in the transverse plane wave, we have

$$\tilde{E}(\tilde{x},\tilde{y},\tilde{z},\tilde{t})=R_0A(x,y,z,t)e^{i(\omega\tilde{t}-n_0k\tilde{z})};\qquad R_0\in\mathbb{R}, \tag{7a}$$

where $\omega$ is the frequency of the light wave, $k$ is the free-space wavenumber of the light wave, and $R_0$ is a scaling factor to be determined later. We choose our variable scalings so that $A$ is an amplitude (envelope) function that is slowly varying in both space and time, compared to the carrier wave multiplying it. Hence, we take

$$x=\varepsilon_x n_0k\tilde{x},\quad y=\varepsilon_y n_0k\tilde{y},\quad z=\varepsilon_z n_0k\tilde{z},\quad t=\varepsilon_t\omega\tilde{t}, \tag{7b}$$

where each of the $\varepsilon_{(\cdot)}$ are small parameters. $\varepsilon_x$ and $\varepsilon_y$ will be dictated by the wavelength of perturbations in the transverse directions. In contrast, $\varepsilon_z$ represents the wavelength of the response in the $z$ direction to those transverse perturbations. As such, it will be determined later when balancing terms in the amplitude equation. The changes to the refractive index are caused by the variance in the amplitude; hence, we have that $n$ depends on the slow time scale $t$, not the fast time scale $\tilde{t}$. (A schematic of all the time scales in the problem is shown in Fig. 3.)

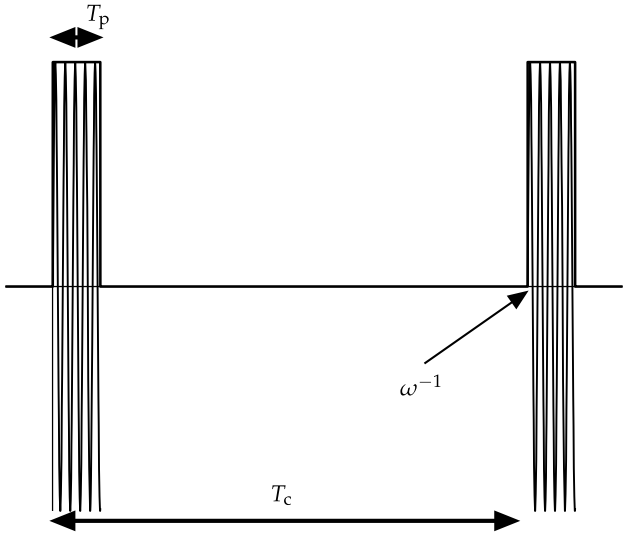


**Fig. 3.** Schematic of various time scales. $T_n$ as defined in Eq. (17) is several orders of magnitude larger than $T_c$.

Substituting Eq. (7) into Eq. (6) and rearranging yields

$$\begin{aligned}\frac{\omega^2}{c^2}\Bigg\{&\varepsilon_t^2\left[(n_0^2+2n_0\delta n)\frac{\partial^2A}{\partial t^2}+2\frac{\partial A}{\partial t}\frac{\partial(2n_0\delta n)}{\partial t}+A\frac{\partial^2(2n_0\delta n)}{\partial t^2}\right]\\&+2i\varepsilon_t\left[(n_0^2+2n_0\delta n)\frac{\partial A}{\partial t}+A\frac{\partial(2n_0\delta n)}{\partial t}\right]-A(n_0^2+2n_0\delta n)\Bigg\}\\&=n_0^2k^2\left(\varepsilon_x^2\frac{\partial^2A}{\partial x^2}+\varepsilon_y^2\frac{\partial^2A}{\partial y^2}\right)+n_0^2k^2\left(\varepsilon_z^2\frac{\partial^2A}{\partial z^2}-2i\varepsilon_z\frac{\partial A}{\partial z}-A\right)\\&+2n_0k^2\varepsilon_x^2\frac{\partial}{\partial x}\left(A\frac{\partial(\delta n)}{\partial x}\right).\end{aligned} \tag{8}$$

Note here that $k$ as defined relates to the variation of the incoming plane wave in vacuum so we have $k=\omega/c$. Keeping only the leading-order terms in each of the $\varepsilon$ variables, we have

$$2i\left(\varepsilon_z\frac{\partial A}{\partial z}+\varepsilon_t\frac{\partial A}{\partial t}\right)=\varepsilon_x^2\frac{\partial^2A}{\partial x^2}+\varepsilon_y^2\frac{\partial^2A}{\partial y^2}+\frac{2\delta nA}{n_0}, \tag{9}$$

where we have used the fact that $\delta n \ll 1$. We absorb the initial amplitude into $R_0$ and pose the problem of Eq. (9) in the region $z \geq 0$ with boundary condition

$$A(x,y,0,t)=1. \tag{10}$$

Experiments suggest that two-photon processes are important in the compaction process; hence, we assume that the relative compaction scales with the total "two-photon dose" $\tilde{D}$ [3,5,8]:

$$\frac{\delta\rho}{\rho}=\kappa\tilde{D}^b,\qquad \tilde{D}=\frac{I_e^2N}{T_p}, \tag{11}$$

where $I_e$ is the fluence of a single pulse, $N$ is the number of pulses, $T_p$ is the duration of the pulse, $b$ is an exponent determined experimentally, and $\kappa$ is a constant of proportionality.

The fluence $I_e$ of each pulse is approximately the product of the irradiance $I_p$ for that pulse and the temporal width $T_p$ of the pulse. Therefore, substituting this result into Eq. (11), we would have $\tilde{D}=I_p^2NT_p$ for $N$ pulses of constant intensity. To better account for the time-varying irradiance of each pulse, we use a Riemann sum in the limit of infinitely many pulses of infinitesimally small duration to obtain

$$\tilde{D}=\lim_{N\to\infty}\sum_{j=1}^{N}\tilde{I}^2(\tilde{t}_j)(\Delta\tilde{t})_j=\int_0^{\tilde{t}}\tilde{I}^2(\tilde{t}')\mathrm{d}\tilde{t}', \tag{12}$$

where we have dropped the subscript "p" to emphasize that we are considering the case of time-varying irradiance.

We associate the amplitude scaling $R_0$ with the irradiance $I_0$ obtained by distributing each pulse's two-photon dose evenly throughout the pulse separation window $T_c$, i.e., by imposing the same dose under a 100% duty cycle. In other words,

$$I_0^2=\frac{I_p^2T_p}{T_c}=\frac{I_e^2}{T_pT_c}, \tag{13}$$

where we rewrite in terms of $I_e$ since it is the quantity commonly given in the literature.

The relationship between intensity and the electric field is given by [9, section 9.2.3]

$$\tilde{I} = \frac{cn\epsilon_0}{2}|\tilde{E}|^2, \tag{14a}$$

where $\epsilon_0$ is the permittivity of vacuum. This motivates the following relationship between $I_0$ and $R_0$:

$$I_0 = \frac{cn\epsilon_0}{2}R_0^2 \Rightarrow \tilde{I}^2(\tilde{t}) = I_0^2|A(\tilde{t})|^4, \tag{14b}$$

where we have used Eq. (7a). Substituting Eq. (14b) into Eq. (12), we have

$$\tilde{D} = I_0^2 T_n D, \qquad D = \int_0^{t_n} |A(t')|^4 \mathrm{d}t', \qquad t_n = \frac{\tilde{t}}{T_n}, \tag{15}$$

where $T_n$ is a characteristic time scale chosen to balance the $\delta n$ term in Eq. (9) with the terms on the left-hand side. (In other words, $T_n$ should be the time scale on which the $\delta n$ terms become important and refractive index changes occur.) Note that as the dose depends on the time-averaged fluence, we do not expect it to be affected greatly by pulse-to-pulse fluctuations.

The constitutive relationship between $\rho$ and $n$ is given by [7]

$$\frac{\delta n}{n_0} = \alpha\frac{\delta\rho}{\rho} \Rightarrow \frac{\delta n}{n_0} = \alpha\kappa(I_0^2 T_n D)^b, \tag{16}$$

where $\alpha$ is a constant, and we have used Eqs. (11) and (15). We want the $\delta n$ term in Eq. (9) to balance with the terms on the left-hand side so we set $\delta n = n_0\varepsilon_z D^b$, which implies that

$$T_n = \frac{1}{I_0^2}\left(\frac{\varepsilon_z}{\alpha\kappa}\right)^{1/b}. \tag{17}$$

Substituting Eqs. (16) and (17) into Eq. (9), we obtain the following final governing equation for $A$:

$$2i\left(\varepsilon_z\frac{\partial A}{\partial z} + \varepsilon_t\frac{\partial A}{\partial t}\right) = \varepsilon_x^2\frac{\partial^2 A}{\partial x^2} + \varepsilon_y^2\frac{\partial^2 A}{\partial y^2} + 2\varepsilon_z D^b A. \tag{18}$$

Note that Eq. (18) is of an unusual form: a nonlinear partial integrodifferential equation, due to the inclusion of a linear history-dependent term $D$. This term is critical, as it models the accumulation of the two-photon dose over time and its accompanying damage to the silica.

## 3. LINEARIZATION OF QUASI-STEADY CASE WITH NO EXPLICIT TIME

As a first approximation, we assume that $\varepsilon_t \ll \varepsilon_z$ so the first-order time derivative in Eq. (18) may be neglected, yielding

$$2i\varepsilon_z\frac{\partial A}{\partial z} = \varepsilon_x^2\frac{\partial^2 A}{\partial x^2} + \varepsilon_y^2\frac{\partial^2 A}{\partial y^2} + 2\varepsilon_z D^b A. \tag{19}$$

We perform a linear stability analysis on transverse perturbations from the plane wave. Hence, we assume a solution of the form

$$A(x, y, z, t) = A_0(z, t)[1 + \varepsilon A_1(x, y, z, t)], \tag{20}$$

where $\varepsilon$ is a small parameter characterizing the size of the perturbations.

Substituting Eq. (20) into Eq. (19) yields to leading orders

$$2i\varepsilon_z\frac{\partial}{\partial z}\{A_0[1 + \varepsilon A_1]\} = \varepsilon A_0\left(\varepsilon_x^2\frac{\partial^2 A_1}{\partial x^2} + \varepsilon_y^2\frac{\partial^2 A_1}{\partial y^2}\right) + 2\varepsilon_z\{(D^b)_0 A_0 + \varepsilon[(D^b)_0 A_0 A_1 + (D^b)_1 A_0]\}, \tag{21a}$$

where we have introduced the notation

$$[D(A_0(1 + \varepsilon A_1))]^b = (D^b)_0 + \varepsilon(D^b)_1 + O(\varepsilon^2), \tag{21b}$$

where the exact forms for $(D^b)_0$ and $(D^b)_1$ differ between cases and will be defined subsequently. Note that for Eq. (21a) to be valid, $\varepsilon$ must be large enough for any terms involving $\varepsilon$ in Eq. (21a) to be larger than any terms neglected in going from Eq. (8) to Eq. (9), i.e., $\max\{\varepsilon_t, \varepsilon_z, \varepsilon_x^2, \varepsilon_y^2\} \ll \varepsilon \ll 1$.

Expanding out the terms at each order, we obtain at $O(1)$

$$i\frac{\partial A_0}{\partial z} = (D^b)_0 A_0, \qquad A_0(0, t) = 1, \tag{22}$$

while at $O(\varepsilon)$, we obtain the following:

$$2i\varepsilon_z\frac{\partial A_1}{\partial z} = \varepsilon_x^2\frac{\partial^2 A_1}{\partial x^2} + \varepsilon_y^2\frac{\partial^2 A_1}{\partial y^2} + 2\varepsilon_z(D^b)_1. \tag{23}$$

Now we consider the *quasi-steady* case. In this case, we assume that $A$ varies slowly with respect to the $t_n$ time scale, so we may treat $|A|$ in Eq. (15) as a constant, yielding

$$D(A) = |A|^4 t_n. \tag{24}$$

With this result, we see from Eq. (22) that $A_0$ is independent of $t$, so we let

$$A_0(z, t) = r_0(z)e^{i\theta_0(z)}, \qquad r_0(0) = 1, \qquad \theta_0(0) = 0, \tag{25}$$

in Eq. (22) to obtain

$$i\frac{dr_0}{dz} - \frac{d\theta_0}{dz}r_0 = (D^b)_0 r_0. \tag{26}$$

We see from Eq. (24) that the right-hand side of Eq. (26) is real so $dr_0/dz = 0$, and

$$r_0(z) = 1 \Rightarrow D(A_0) = t_n, \tag{27a}$$

where we have used Eq. (24). Next, substituting Eq. (27a) into the real part of Eq. (26), we have

$$\theta_0 = -t_n^b z. \tag{27b}$$

Since the problem (at this order) has no transverse variation, we have no focusing but just a phase shift that increases in $z$. Using these results, we obtain

$$(D^b)_1 = 2bt_n^b(A_1 + \overline{A_1}).$$

Since $(D^b)_1$ is real, we must use a pair of transverse complex exponentials to perturb the plane wave as follows:

$$A_1(x, y, z, t) = A_+(z, t)\Phi(x, y) + A_-(z, t)\overline{\Phi(x, y)},$$
$$\Phi(x, y) = e^{i(x+y)}, \tag{28}$$

where the wavenumber of the transverse perturbations has been absorbed into the scaling. Substituting Eq. (28) into Eq. (23), we obtain

$$2i\varepsilon_z\frac{\partial A_+}{\partial z}\Phi = (-\varepsilon_x^2 - \varepsilon_y^2)A_+\Phi + 2\varepsilon_z[2bt_n^b(A_+\Phi + \overline{A_+\Phi})]. \tag{29}$$

Equation (29) yields a natural physical spatial scale to determine $\varepsilon_z$. In particular, if we choose

$$\varepsilon_z = \frac{\varepsilon_x^2 + \varepsilon_y^2}{2}, \tag{30}$$

then all of the terms in Eq. (29) will balance. This scaling is characteristic of fields evolving under the paraxial approximation. The actual transverse spatial scales are likely selected by

nonlinear terms at $O(\varepsilon^2)$, but this is beyond the scope of the paper.

To verify this scaling, we examine typical parameter values from the literature, as shown in Table 1. The final column shows the parameters used in the paper. Most are from Wright [7]; in the two exceptions, the parameter values were provided by an industrial representative working in the area.

By rewriting our definition for $\varepsilon_z$ in terms of wavelengths $\lambda_{(\cdot)} = 2\pi k_{(\cdot)}$, we have

$$\varepsilon_z = \frac{\lambda^2}{2n_0^2(\lambda_x^2 + \lambda_y^2)} = 1.66 \times 10^{-6},$$

which is small, as theorized. Moreover, the normalization scale for $z$ is given by $(\varepsilon_z n_0 k)^{-1} = 1.23$ cm, a length scale along which the damage can be seen [5].

We may also use the values to confirm our interpretation of $T_n$ as the time scale on which refractive index changes occur. Using the values in Table 1, we obtain $T_n = 6.80 \times 10^2$ s, or around $6.8 \times 10^5$ pulses. In Wright [7], they observe their first "hot spots" around $6 \times 10^6$ pulses, which verifies that this normalization provides the right order of magnitude.

With the confidence in our scalings that the experimental measurements provide, we substitute Eq. (30) into Eq. (23) and use the replacement in Eq. (28) to obtain the following:

$$i\left(\frac{\partial A_+}{\partial z}\Phi + \frac{\partial A_-}{\partial z}\bar{\Phi}\right) = -A_+\Phi + 2bt_n^b(A_+\Phi + \overline{A_+\Phi} + A_-\bar{\Phi} + \overline{A_-\bar{\Phi}}). \quad (31)$$

The PDE Eq. (31) is actually an ODE in $z$ parametrized by $t_n$ so we replace $\partial$ with $d$ in the subsequent analysis. Collecting coefficients of the positive and negative exponentials, we have

$$i\frac{dA_+}{dz} = -A_+ + 2bt_n^b(A_+ + \overline{A_-}), \quad (32a)$$

$$-i\frac{d\overline{A_-}}{dz} = -\overline{A_-} + 2bt_n^b(\overline{A_-} + A_+), \quad (32b)$$

where in the last line we have taken the complex conjugate so we have a system in $\{A_+, \overline{A_-}\}$.

To solve Eqs. (32), we assume that

$$A_+ = \gamma_+ e^{i\mu z}, \qquad \overline{A_-} = \gamma_- e^{i\mu z}, \quad (33)$$

and find the eigenvalues $\mu$. Substituting Eq. (33) into Eqs. (32), we have

$$\gamma_+(\mu + 2bt_n^b - 1) + 2bt_n^b\gamma_- = 0,$$
$$2bt_n^b\gamma_+ + \gamma_-(-\mu + 2bt_n^b - 1) = 0, \quad (34)$$

which has a nontrivial solution only when

$$\mu = \pm\sqrt{1 - 4bt_n^b}. \quad (35)$$

At $t_n = 0$, $\mu = \pm 1$, which is consistent with our choice of length scale in Eq. (30). However, for $t_n > (4b)^{-1/b}$, the eigenvalues become imaginary, which causes exponential growth in $z$. Note that the maximal amplitude will be at the end furthest from the beam, as seen experimentally [1]. Using the parameters in Table 1, we state that the transition occurs at $t_n = 1/4$, or around 3 min, which is on the same order as experimental results.

## 4. LINEARIZATION OF UNSTEADY CASE WITH NO EXPLICIT TIME

Next we consider the more realistic case where $t_n = t$. However, we still assume that $\varepsilon_t \ll \varepsilon_z$ so we neglect the $\partial/\partial t$ term in Eq. (18). In that case, we may follow the analysis in Section 3, but we keep the full form of $D$ in Eq. (15). Nevertheless, since $D^b$ is still real, Eqs. (27) hold with $t_n$ replaced by $t$.

In this case, we may expand our expression for $D^b$ to yield

$$D^b = \left[\int_0^t 1 + 2\varepsilon(A_1 + \overline{A_1})\mathrm{d}t'\right]^b \quad (36a)$$

$$\sim t^b\left(1 + \frac{2b\varepsilon}{t}\int_0^t A_1 + \overline{A_1}\mathrm{d}t'\right),$$

$$(D^b)_1 = 2bt^{b-1}\int_0^t A_1 + \overline{A_1}\mathrm{d}t'. \quad (36b)$$

Again $(D^b)_1$ is real, so we must use both $A_+$ and $A_-$ in our analysis, as in Section 3. Substituting Eqs. (36b) and (28) into Eq. (23), we have

$$i\frac{\partial}{\partial z}(A_+\Phi + A_-\bar{\Phi}) = -(A_+\Phi + A_-\bar{\Phi}) + 2bt^{b-1}\int_0^t A_+\Phi + A_-\bar{\Phi} + \overline{A_+\Phi + A_-\bar{\Phi}}\mathrm{d}t', \quad (37)$$

**Table 1. Parameter Values from the Literature**

| | Reference | | | | |
|---|---|---|---|---|---|
| Parameter | Borrelli [5] | Piao [2] | Primak [3,8] | Wright [7] | Used |
| $b$ | 0.5–0.7 | 2/3 | 2/3 | 0.5 | 0.5 |
| $f_c = (T_c)^{-1}$(Hz) | | 330 | | | 1000 |
| $n_0$ | | | | 1.5 | 1.5 |
| $I_e$ (mJ/(cm$^2$ · pulse)) | | 10–20 | | 50 | 50 |
| $T_p$ (ns/pulse) | | 30 | | 20 | 20 |
| $\alpha$ | | | | 0.3 | 0.3 |
| $\kappa$ [$10^{-6}$(cm$^4$ · ns/($10^6$ mJ$^2$))$^b$] | | 0.916–1.45 | | 0.6 | 0.6 |
| $\lambda$ (μm) | | | | 0.193 | 0.193 |
| $\lambda_x, \lambda_y$ (μm) | | | | | 50 |

where we have used Eq. (30). Equation (37) is analogous to Eq. (31). Hence, we again separate coefficients of the positive and negative exponentials to obtain

$$i\frac{\partial A_+}{\partial z} = -A_+ + 2bt^{b-1}\int_0^t A_+ + \overline{A_-}\,\mathrm{d}t', \tag{38a}$$

$$-i\frac{\partial \overline{A_-}}{\partial z} = -\overline{A_-} + 2bt^{b-1}\int_0^t \overline{A_-} + A_+\,\mathrm{d}t'. \tag{38b}$$

In the case where $A_-$ and $A_+$ are constant, Eqs. (38) reduce to Eqs. (32) with $t$ replacing $t_n$. The above analysis assumes that $D^b$ is $O(1)$, and is therefore not valid if $t = O(\varepsilon)$.

The form of the normal modes is more complicated; we try functions of the form

$$A_+ = \gamma_+ e^{i\mu z}F(t), \qquad \overline{A_-} = \gamma_- e^{i\mu z}F(t), \tag{39}$$

where $F(t)$ is to be determined. Substituting Eq. (39) into Eq. (38a) yields the following:

$$(\mu - 1)\gamma_+ F(t) + 2bt^{b-1}(\gamma_+ + \gamma_-)\int_0^t F(t')\mathrm{d}t' = 0. \tag{40}$$

In order for this to reduce to an algebraic equation, we must have the $F(t)$ terms cancel, so

$$F(t) = \frac{bt^{b-1}}{\phi}\int_0^t F(t')\mathrm{d}t', \qquad \phi = \frac{(1-\mu)\gamma_+}{2(\gamma_+ + \gamma_-)}.$$

Solving this equation, we have

$$F(t) = F_0 t^{b-1}e^{t^b/\phi}. \tag{41}$$

We recall from our previous discussion that Eq. (21b) does not hold as $t \to 0$; hence, neither does Eq. (41). (In fact, $F$ diverges as $t \to 0$, which also causes our expansion to break down.) These results suggest the presence of an initial layer. An analytical study of the solution in this layer is beyond the scope of the current work, but we define $F_0$ as the constant required to asymptotically match our solution to the initial-layer solution.

Repeating this analysis using Eq. (38b) yields

$$\phi = \frac{(1+\mu)\gamma_-}{2(\gamma_+ + \gamma_-)}.$$

Compatibility between the two expressions for $\phi$ requires that

$$(1-\mu)\gamma_+ = (1+\mu)\gamma_-.$$

Thus,

$$\phi = \frac{1-\mu^2}{4}, \tag{42}$$

which has solutions for all positive $\mu$ so there are always oscillations in $z$. For $\mu < 1$ (which corresponds to low frequencies), $\phi > 0$, which corresponds to exponential growth in time. We note from Eq. (41) that the fastest-growing mode has $\phi \to 0^+$, which corresponds to $\mu \to 1^-$.

The mode $\mu = 1$ corresponds to the normalization length scale

$$(\varepsilon_x n_0 k)^{-1} = k_x^{-1} = \frac{\lambda_x}{2\pi},$$

and hence the fastest growing mode corresponds to the assumed scale of the transverse perturbations. Again, this length scale is comparable to the one on which damage is seen [1].

## 5. EXPLICIT TIME DEPENDENCE

We return to the consideration of the quasi-steady case, but now we include the $\partial/\partial t$ term in Eq. (18) by taking $\varepsilon_t = \varepsilon_z/c_\varepsilon$, where $c_\varepsilon = O(1)$. Therefore, Eq. (18) is replaced by

$$2i\varepsilon_z\left(\frac{\partial A}{\partial z} + \frac{1}{c_\varepsilon}\frac{\partial A}{\partial t}\right) = \varepsilon_x^2\frac{\partial^2 A}{\partial x^2} + \varepsilon_y^2\frac{\partial^2 A}{\partial y^2} + 2\varepsilon_z D^b A. \tag{43}$$

However, by defining

$$\tau = t - \frac{z}{c_\varepsilon}, \tag{44}$$

and writing $A(x, y, z, t)$ as $A(x, y, z, \tau)$, we have

$$2i\varepsilon_z\frac{\partial A}{\partial z} = \varepsilon_x^2\frac{\partial^2 A}{\partial x^2} + \varepsilon_y^2\frac{\partial^2 A}{\partial y^2} + 2\varepsilon_z D^b A,$$

which is just Eq. (19). Therefore, all our results from Section 3 hold with $t$ replaced by $\tau$ since in this case $D$ is independent of $t$.

In the unsteady case where $D$ does depend on $t$, we substitute Eq. (20) into Eq. (43) to obtain, to leading two orders,

$$i\left(\frac{\partial A_0}{\partial z} + \frac{1}{c_\varepsilon}\frac{\partial A_0}{\partial t}\right) = (D^b)_0 A_0, \tag{45a}$$

$$2i\varepsilon_z\left(\frac{\partial A_1}{\partial z} + \frac{1}{c_\varepsilon}\frac{\partial A_1}{\partial t}\right) = \varepsilon_x^2\frac{\partial^2 A_1}{\partial x^2} + \varepsilon_y^2\frac{\partial^2 A_1}{\partial y^2} + 2\varepsilon_z(D^b)_1, \tag{45b}$$

analogous to Eqs. (22) and (23). For this problem, we need the following boundary and initial conditions:

$$A_0(0, t) = 1, \qquad A_0(z, 0) = 0. \tag{46}$$

We may posit a solution of the form in Eq. (25), but in this case both $r_0$ and $\theta_0$ must be functions of time. Therefore, we have

$$A_0(z, t) = r_0(z, t)e^{i\theta(z,t)},$$
$$r_0(0, t) = 1, \qquad \theta_0(0, t) = 0, \qquad r_0(z, 0) = 0, \tag{47}$$

where we have used Eq. (46). Substituting Eq. (47) into Eq. (45a), we obtain

$$i\left(\frac{\partial r_0}{\partial z} + \frac{1}{c_\varepsilon}\frac{\partial r_0}{\partial t}\right) - \left(\frac{\partial \theta_0}{\partial z} + \frac{1}{c_\varepsilon}\frac{\partial \theta_0}{\partial t}\right)r_0 = (D^b)_0 r_0, \tag{48}$$

analogous to Eq. (26).

With the definition of $D$ in Eq. (15), the right-hand side of Eq. (48) is still real, so the imaginary part of Eq. (48) is

$$\frac{\partial r_0}{\partial z} + \frac{1}{c_\varepsilon}\frac{\partial r_0}{\partial t} = 0 \Rightarrow r_0(z, t) = r_0(z - c_\varepsilon t) = \begin{cases} 1, & z < c_\varepsilon t, \\ 0, & z > c_\varepsilon t, \end{cases}$$

where we have used the initial and boundary conditions in Eq. (47). Continuing to simplify, we obtain

$$r_0(z, t) = H(c_\varepsilon t - z) \Rightarrow r_0(z, \tau) = H(\tau), \tag{49}$$

where $H(\cdot)$ is the Heaviside function.

Substituting Eq. (49) and the definition of $D$ into the real part of Eq. (48), we have

$$\left(\frac{\partial\theta_0}{\partial z}+\frac{1}{c_\varepsilon}\frac{\partial\theta_0}{\partial t}\right)=-H(c_\varepsilon t-z)\left(t-\frac{z}{c_\varepsilon}\right)^b. \tag{50}$$

Next, writing $\theta_0$ as a function of $\tau$ and using Eq. (44), we obtain the following:

$$\frac{\partial\theta_0}{\partial z}=-\tau^b H(\tau);\quad \theta(0,\tau)=0$$
$$\theta_0(z,\tau)=-\tau^b H(\tau)z, \tag{51}$$

where we have used Eq. (47). Equation (51) is Eq. (27b) with $t$ replaced by $\tau$, multiplied by $H(\tau)$.

Continuing our analysis, we compute $(D^b)_1$ in the case where $A_0$ is not constant by examining

$$D^b\sim H(\tau)\left[\int_0^\tau 1+2\varepsilon(A_1+\overline{A_1})\mathrm{d}\tau\right]^b, \tag{52}$$

which is essentially the same as Eq. (36a) with $t$ replaced by $\tau$. Hence, writing $A_1(x,y,z,t)$ as $A_1(x,y,z,\tau)$ and using Eq. (44), Eq. (45b) becomes

$$2i\varepsilon_z\frac{\partial A_1}{\partial z}=\varepsilon_x^2\frac{\partial^2 A_1}{\partial x^2}+\varepsilon_y^2\frac{\partial^2 A_1}{\partial y^2}+2\varepsilon_z(D^b)_1(\tau),$$

where we have explicitly written the dependence of $(D^b)_1$ on $\tau$. This is just Eq. (23) with $t$ replaced by $\tau$. Therefore, our analysis in Section 4 holds with $t$ replaced by $\tau$.

Thus, we have shown that in both cases of interest, retaining the $\partial/\partial t$ term in Eq. (18) simply introduces a variable shift.

## 6. CONCLUSIONS AND FURTHER RESEARCH

When using fused silica lenses for photolithography and other applications, it is critical to maintain the optical integrity of the lens for as long as possible. The desire for finer beam control has led to the use of smaller wavelengths in the UV range. Unfortunately, these wavelengths correspond to higher intensities, which increase the two-photon dosage imparted by the beam. The increased dosage, in turn, yields to compaction or densification of the lens, and eventually the formation of microchannels.

To model this situation, we employed Maxwell's equations with an index of refraction that depended on the electric field. In the case of small perturbations from the plane wave, spatial variations in the index of refraction could be neglected. The resulting nonlinear partial integrodifferential equation for the amplitude models the cumulative effects of the two-photon absorption through the term $D$. The theory for the dose–compaction relationship was established in [3,5,8].

We examined the case of a slightly perturbed plane wave moving through the fused silica. The leading-order solution satisfies both the linear and nonlinear terms. The inclusion of transverse perturbations leads to a linear stability analysis, where the paraxial approximation is shown to hold.

We examined both the quasi-steady case, where the dosage is assumed to be occurring on a different time scale from the slowly varying amplitude, and the unsteady case, where both processes are assumed to occur on the same time scale. We began by considering the case where the explicit time dependence is suppressed.

In the quasi-steady case, the stability analysis leads to an estimate for the time at which the modes become unsteady and begin to grow exponentially in space. This time compares favorably with experimental and simulated results and the solution profile, with maximal amplitude at the exit face. As large gradients in intensity produce a strong electrostrictive force out of the back face [7], these results are consistent with experimental observations of microchanneling, especially considering that surface damage thresholds are smaller than those in the bulk.

In the unsteady case, the form of the time-dependent eigenfunctions is more complicated. We derived expressions that hold away from an initial layer. In this analysis, the growth rate of the mode depends on its wavelength, with the fastest growth rate occurring for $\mu$ near 1, or on the typical transverse perturbation wavelength.

We concluded with the case where the time derivative in Eq. (18) is explicitly included. This simply introduces a change of variable in the problem, as all our previous results held with $t$ replaced by the shifted time variable $\tau$.

Our results demonstrate that the nonlinear constitutive relation Eq. (16) is robust enough to model the growth in amplitude perturbations associated with the compaction phenomenon, even in the relatively straightforward case of a slowly varying plane wave. They also demonstrate directly the dependence of the solution on the physical parameters in the problem.

**Funding.** National Science Foundation (NSF) (DMS-1261592, DMS-1261596).

**Acknowledgment.** This paper grew out of a problem at the 30th Annual Workshop on Mathematical Problems in Industry. We particularly thank Thomas P. Witelski of Duke University for helpful contributions to this work and Leslie Button of Corning for many useful comments.

## REFERENCES

1. A. Burkert, W. Triebel, U. Natura, and R. Martin, "Microchannel formation in fused silica during ArF excimer laser irradiation," Phys. Chem. Glasses: Eur. J. Glass Sci. Technol. B **48**, 107–112 (2007).
2. F. Piao, W. G. Oldham, and E. E. Haller, "Ultraviolet-induced densification of fused silica," J. Appl. Phys. **87**, 3287–3293 (2000).
3. W. Primak, "Dependence of the compaction of vitreous silica on the ionization dose," J. Appl. Phys. **49**, 2572 (1977).
4. A. Ghatak and K. Thyagarajan, *An Introduction to Fiber Optics* (Cambridge University, 1998).
5. N. F. Borrelli, C. Smith, D. C. Allan, and T. P. Seward III, "Densification of fused silica under 193-nm excitation," J. Opt. Soc. Am. B **14**, 1606–1615 (1997).
6. I. S. Gradshteĭn and I. M. Ryzhik, *Table of Integrals, Series, and Products*, 5th ed. (Academic, 1994).
7. E. M. Wright, M. Mansuripur, V. Liberman, and K. Bates, "Spatial pattern of microchannel formation in fused silica irradiated by nanosecond ultraviolet pulses," Appl. Opt. **38**, 5785–5788 (1999).
8. W. Primak and R. Kampwirth, "The radiation compaction of vitreous silica," J. Appl. Phys. **39**, 5648–5651 (1968).
9. D. Griffiths, *Introduction to Electrodynamics*, 4th ed. (Pearson Education, 2012).